

**Original citation:**

Chote, Paul and Sullivan, D. J.. (2016) The post-outburst pulsations of the accreting white dwarf in the cataclysmic variable GW Librae. Monthly Notices of the Royal Astronomical Society, 458 (2). pp. 1393-1401

**Permanent WRAP URL:**

<http://wrap.warwick.ac.uk/78565>

**Copyright and reuse:**

The Warwick Research Archive Portal (WRAP) makes this work by researchers of the University of Warwick available open access under the following conditions. Copyright © and all moral rights to the version of the paper presented here belong to the individual author(s) and/or other copyright owners. To the extent reasonable and practicable the material made available in WRAP has been checked for eligibility before being made available.

Copies of full items can be used for personal research or study, educational, or not-for profit purposes without prior permission or charge. Provided that the authors, title and full bibliographic details are credited, a hyperlink and/or URL is given for the original metadata page and the content is not changed in any way.

**Publisher's statement:**

This is a pre-copyedited, author-produced PDF of an article accepted for publication in Monthly Notices of the Royal Astronomical Society following peer review. The version of record Chote, Paul and Sullivan, D. J.. (2016) The post-outburst pulsations of the accreting white dwarf in the cataclysmic variable GW Librae. Monthly Notices of the Royal Astronomical Society, 458 (2). pp. 1393-1401. is available online at:

<http://dx.doi.org/10.1093/mnras/stw421>

**A note on versions:**

The version presented here may differ from the published version or, version of record, if you wish to cite this item you are advised to consult the publisher's version. Please see the 'permanent WRAP url' above for details on accessing the published version and note that access may require a subscription.

For more information, please contact the WRAP Team at: [wrap@warwick.ac.uk](mailto:wrap@warwick.ac.uk)

# The post-outburst pulsations of the accreting white dwarf in the cataclysmic variable GW Librae

P. Chote<sup>1,2</sup><sup>★</sup><sup>‡</sup>, D. J. Sullivan<sup>2</sup><sup>†</sup><sup>‡</sup>

<sup>1</sup>*Department of Physics, University of Warwick, Coventry CV4 7AL, United Kingdom*

<sup>2</sup>*School of Chemical & Physical Sciences, Victoria University of Wellington, P.O. Box 600, Wellington, New Zealand*

## ABSTRACT

We present new time-series photometry of the accreting pulsating white dwarf system GW Librae obtained in 2012 and 2013 at the University of Canterbury Mt John Observatory in New Zealand. Our 2012 data show the return of a  $\sim 19$  minute periodicity that was previously detected in 2008. This pulsation mode was a dominant feature of our quality May 2012 data set, which consisted of six contiguous nights; a detailed analysis indicated a degree of frequency variability. We show by comparison with the previously identified pulsation modes that this periodicity is best explained as a new mode, and that the quasi-stability of the periods appears to be a general feature of the pulsations in these systems. We also find a previously unreported 3-hour modulation period, which we believe to be related to the known two and four hour periods of so far unknown origin.

**Key words:** stars: individual: GW Librae – stars: variables: general – white dwarfs – asteroseismology

## 1 INTRODUCTION

White dwarfs (WDs) are the final evolutionary state of around 98 per cent of stars in our Galaxy. Efficient chemical diffusion in their envelopes due to the high surface gravities produces atmospheres composed predominantly of the lightest elements hydrogen and helium. About 80 per cent of WDs have a hydrogen atmosphere (spectral type DA) overlying a helium zone, and the bulk of the remaining 20 per cent (spectral type DB) have helium atmospheres.

As isolated WDs slowly cool they pass through temperature regimes in which nonradial  $g$ -mode pulsations are observable. For the DA WDs the instability strip occurs near  $T_{\text{eff}} \sim 12$  kK in which a partially ionized H layer in the envelope drives the pulsations (Dziembowski & Koester 1981; Brickhill 1991). The DB instability strip occurs in a significantly higher and less well-defined temperature regime ( $T_{\text{eff}} \sim 23 - 28$  kK) as the driving mechanism involves a partially ionized He I layer in the outer regions (Winget et al. 1982). This temperature uncertainty is primarily due to the difficulty of establishing a  $T_{\text{eff}}$  value based on the largely temperature-independent behaviour of the He I spectral lines in the temperature interval (Bergeron et al. 2011; Chote et al. 2013).

The nonradial pulsations are of low spherical harmonic order, have periods  $\sim 10^2 - 10^3$  s, and involve largely horizontal material displacements along gravitational equipotential surfaces. This creates surface temperature oscillations, leading to observable flux variations.

The eigenfrequencies of these pulsations provide a fingerprint of the internal structure of the WD, and if enough modes are detected asteroseismic techniques can be employed to extract measurements of basic properties such as the size of the degenerate core of the WD, rotation rates, and the mass, depth, and convection zone properties of the helium and hydrogen layers in their envelopes (see e.g. Winget & Kepler 2008; Fontaine & Brassard 2008; Althaus et al. 2010, for comprehensive reviews on the field).

Both the period and shape of the luminosity variations associated with a pulsation mode change as a function of temperature (Mukadam et al. 2006), but because isolated WDs evolve very slowly through the instability strips, we are limited to probing a single snapshot in an individual star’s evolution. The DAVs evolve at the slowest rate ( $dP/dt \sim 10^{-15}$  s s<sup>-1</sup>; e.g. Kepler et al. 2005; Mukadam et al. 2013; Sullivan & Chote 2015), while the hotter DBVs, unsurprisingly, are expected to evolve more rapidly (Winget et al. 2004).

A small number of systems, of which GW Librae (GW Lib) is the prototypical member, feature a pulsating WD that is accreting material from a close companion star via an accretion disk. These systems (which exist as a sub-group of the Cataclysmic Variables) undergo out-

★ E-mail: p.chote@warwick.ac.uk

† Email: denis.sullivan@vuw.ac.nz

‡ Visiting Astronomer, University of Canterbury Mt John Observatory

bursts when the accretion disk reaches a critical density, becomes thermally unstable, and rapidly dumps material onto the WD. The conversion of gravitational potential energy to heat raises the surface temperature of the WD to a few thousand Kelvin above the instability strip, and the pulsations cease. Over the following few years the pulsations return and evolve as the WD cools back towards its pre-outburst temperature (Piro et al. 2005).

These systems have a low accretion rate, and so the WD dominates the visible and ultraviolet luminosity (estimated as  $\gtrsim 60$  per cent for GW Lib in the *V* band (Vican et al. 2011)) when the system is not undergoing an outburst. This makes it possible to detect the intrinsic luminosity variations generated by the pulsations during the long quiescent periods between outbursts ( $\gtrsim 10$  years).

A side effect of the accretion is that the WD envelope composition is contaminated with helium and other elements from the companion star. This creates a more complicated parameter space in which pulsations may be driven over a wider range of temperatures than the traditional DA and DB instability strips (Arras et al. 2006; Van Grootel et al. 2015). The accumulated angular momentum spins the WD up to fast rotation rates (down to a few minutes), which will have an as yet undetermined effect on the pulsations, and is relevant for the discussion of the fast rotating ‘superchandrasekhar’ WDs that have been proposed as Type Ia supernovae candidates (e.g. Yoon & Langer 2005).

GW Lib was the first accreting pulsating WD to be identified, and remains to date the most well studied. Subsequent discoveries have provided  $> 15$  additional systems (see Table 6 of Szkody et al. (2010), plus the more recent discoveries by Pavlenko (2009); Woudt & Warner (2011); Uthas et al. (2012)). The historical time line of the key observational programmes targeting GW Lib and their main results are summarised in Table 1.

## 2 MT JOHN OBSERVATIONS

In 2011 we joined an observational programme to monitor GW Lib as it cooled from its 2007 outburst. We obtained nine runs in 2011 which were originally reported in Szkody et al. (2012). The primary focus of this paper are an additional nine runs that were obtained between March and May 2012 (initially reported in Chote & Sullivan (2013)) plus an additional run obtained in March 2013. The details of these 19 runs are presented in Table 1.

All observations were acquired using the Puokouni high-speed photometer (Chote et al. 2014) with the 1m telescope at the University of Canterbury Mt John Observatory (UCMJO). We used our standard BG40 broad B band filter in order to minimise the sky contributions to the bluer WD flux. The photometer employs a frame transfer CCD, so there were negligible deadtimes involved in the data acquisition. The CCD frames were analysed and light curves extracted using our standard reduction procedure (see Chote et al. 2014) with one change: the per-run polynomial fit to correct for differential extinction is not appropriate for these runs because GW Lib shows intrinsic variability on a similar timescale to the changing extinction ( $\sim$ hours), and it is not possible to separate these effects within a single run. We instead take a different approach, described in Fig.

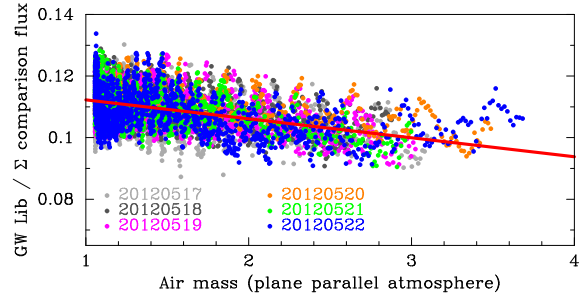


**Figure 1.** The residual extinction in the photometry was modelled and removed from the data by calculating the change in mean relative intensity with increasing air mass. The times associated with each raw target / comparison flux ratio were converted to an air mass (assuming a plane parallel atmosphere), and the flux ratio was simultaneously fitted over the six nights for air masses 1 – 3. The mean intensity of GW Librae remains constant to a level much better than the  $\sim 10\%$  pulsation modulation, which appears in the plot as the large scatter about the mean trend. These variations are averaged over  $\sim 12$  independent measurements (two per night as the field rises and sets) to provide a much more robust extinction correction than the standard per-night polynomial fit.

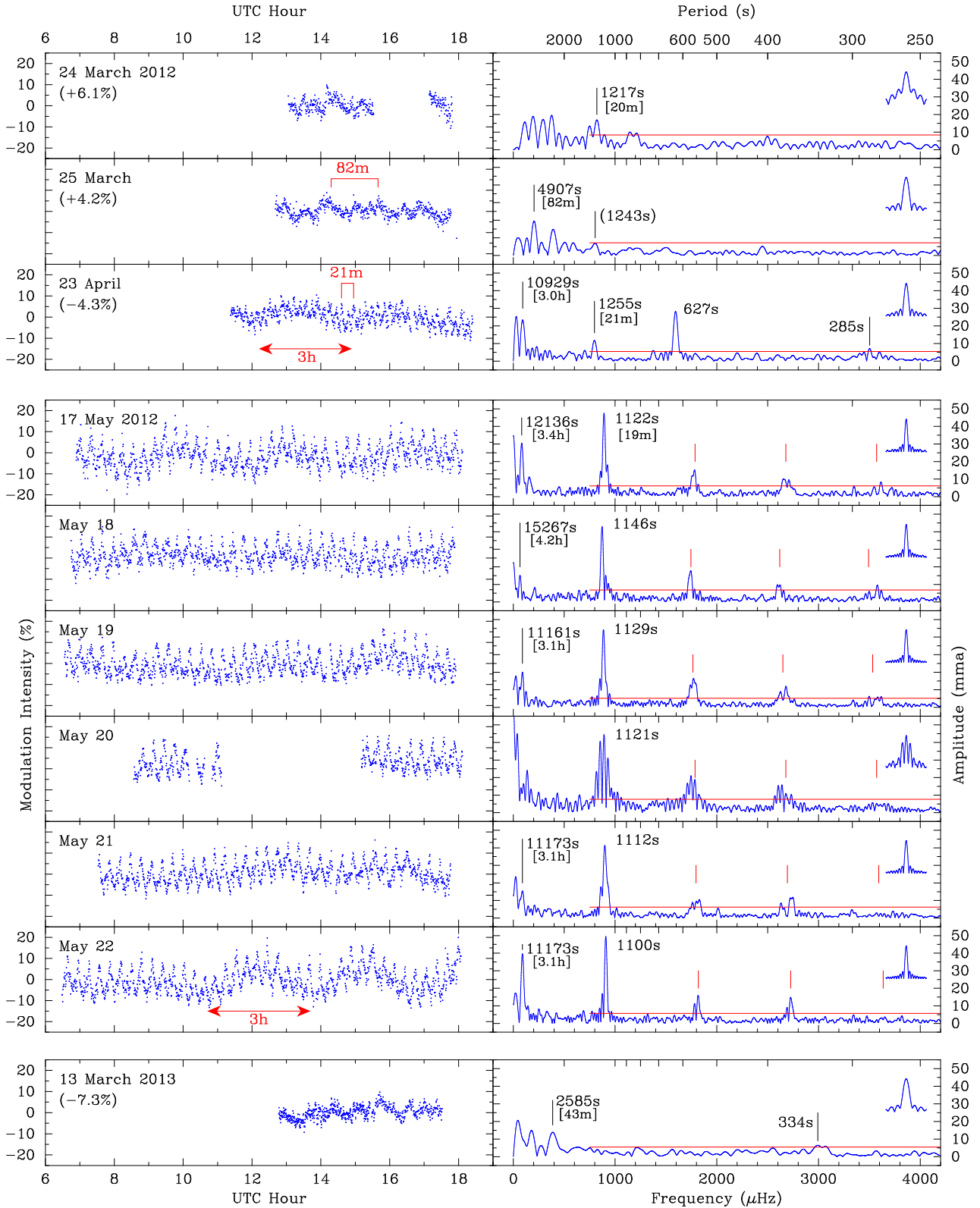
1, that fits an extinction parameter simultaneously to the six 2012 May runs. The extinction parameter from this fit was reused for the 2012 March, April and 2013 April runs.

Fig. 2 presents the reduced time-series and amplitude Fourier Transform (DFT hereon) plots of the new data. Similar plots of the 2011 runs are presented in Figs. 12 and 14 of Szkody et al. (2012). The horizontal (red) lines in the DFT panels indicate the 0.1 per cent false alarm probabilities (FAP; Sullivan et al. 2008), which are calculated using a Monte Carlo process and represent the threshold where there is a 0.1 per cent probability that a peak in the DFT greater than this amplitude may occur by a conspiracy of the random photometric noise. We calculate the FAP for each run over the frequency range  $750 - 10000 \mu\text{Hz}$  after prewhitening the 1100s, 280s, and 3h signals discussed in the following sections. Due to the possible contributions from  $1/f$  noise and other effects our FAP evaluation procedures are less reliable for the longer periods so limit the estimates to greater than  $750 \mu\text{Hz}$ . The reality of the long period variations (e.g. the  $\sim 3$ h modulations) are best viewed in the time domain.

The two March 2012 runs show a  $\sim 80$  minute double-humped modulation, which is longer than both the orbital period and the 78 minute superhump period that was seen during the 2007 outburst (Kato et al. 2008; Bullock et al. 2011). The DFT shows power near 20 minutes, but these peaks are not clearly distinguished.

The April 2012 light curve was dominated by a double-humped 1255 s (21 minute) periodicity superimposed on top of a longer three hour modulation which is discussed in Section 5. The DFT also shows power in the vicinity of the  $\sim 280$ s pulsations seen during 2010 and 2011.

Less than one month later, on 2012 May 17, the 1255 s signal appears to have shifted to a shorter period of  $\sim 1100$ s and roughly doubled in amplitude. This was again superimposed on top of a 3 h modulation. The DFT of this first run showed a clear signal at 1120s and its harmonics, but the peak profile appeared to indicate some underlying frequency structure.



**Figure 2.** The new observational data on GW Lib obtained in 2012 and March 2013 using the Puoko-nui photometer attached to the Mt John 1m telescope. All CCD exposure times were 30 s. The panels on the left depict the flux variations about the mean levels in per cent modulation units, and the panels on the right show the corresponding DFTs for each data set in millimodulation amplitude (mma) units (10 mma = 1 per cent amplitude). The DFT window functions for each run are provided in the panel inserts and have the same horizontal frequency scale. The horizontal (red) lines in the DFT panels represent the False Alarm Probabilities (FAP) at the 1 in 1000 significance level (see text). The vertical (red) lines in the DFT panels indicate the harmonics at 2, 3, 4  $\times$  the noted base frequency. The intensity of the six 2012 May runs are measured relative to a common mean value, which is  $\sim 0.1$  mag fainter (as measured through the BG40 filter) than the 2011 July observation campaign (Szkody et al. 2012). The percentages noted below the dates in the other four panels show the mean intensity difference of these runs relative to 2012 May.

**Table 1.** A brief tabular history of the key observational papers studying GW Librae.

Observation Date		Observations	Reference
Year	Month		
1983	August	First outburst detected: mag $\sim 18 \rightarrow \sim 9$ (nova classification)	Maza & Gonzalez (1983)
1987	–	Spectroscopic classification as dwarf Nova (DN)	Duerbeck & Seitter (1987)
1991	June	Spectroscopic classification as DN of WZ Sge type	Ringwald et al. (1996)
1997	March	Pulsations in white dwarf primary discovered near 390, 650 s	Warner & van Zyl (1998)
1998	April	Spectroscopic measurement of 76.4 min orbital period	Szkody et al. (2000)
1998	May	Multi-site photometry campaign: pulsation periods near 650, 370, 230 s	van Zyl et al. (2004)
1999	June	Refined 76.79 min spectroscopic orbital period determination	Thorstensen et al. (2002)
2001	May	Discovery of an unknown 2.1 h periodicity.	Woudt & Warner (2002)
2002	January	HST observations show large UV pulsation amplitudes and solar-like metals	Szkody et al. (2002)
2002	May	Spectroscopic measurement of 97 s spin period.	van Spaandonk et al. (2010)
2005	May	VLT multicolour observations clearly show pulsations and 2.1 h modulation	Copperwheat et al. (2009)
2007	April	Second outburst detected: peaked at 8 mag	Templeton et al. (2007)
...		Photometric observations by several groups following...	Vican et al. (2011)
...		...the evolution of the outburst and subsequent cooling	Kato et al. (2008)
2007	April	Swift observations show unusual x-ray flux increase during outburst	Byckling et al. (2009)
2007 – 2009		Some photometric variability observed, including a new $\approx 19$ min period...	Copperwheat et al. (2009)
...		...plus 2.1 h & 4 h modulations. No clear evidence for WD pulsations	Vican et al. (2011)
...			Bullock et al. (2011)
2010	March	HST observations detect pulsations	Szkody et al. (2012)
2011	April	Pulsations detected via HST and ground-based observations	Szkody et al. (2012)
2012	May	Photometric study of the 19 minutes WD pulsation	This paper
2013	May	Spectroscopic study of a 3.85 h modulation	Tolosa et al. (2016)

**Table 2.** Table of GW Lib observation runs. All runs were acquired using a BG40 filter with the Puoko-nui instrument on the 1 m telescope at UCMJO.

UT Date	UT Start	Exposure (sec)	Useable Hours	0.1% FAP (mma)
2 Mar 2011	13:09:00	20	4	10.4
4 Mar 2011	14:33:00	20	1.5	11.8
1 Jul 2011	07:02:00	20	5	4.9
2 Jul 2011	06:23:00	20	4.5	4.3
4 Jul 2011	06:36:00	20	7.5	3.8
6 Jul 2011	06:35:00	20	3	6.9
27 Jul 2011	06:48:00	20	5.5	5.8
1 Aug 2011	06:39:00	20	5	5.3
2 Aug 2011	06:35:00	20	3	5.8
24 Mar 2012	13:02:00	30	3.5	8.4
25 Mar 2012	12:40:00	30	5.0	7.2
23 Apr 2012	11:22:00	30	7.0	5.5
17 May 2012	6:53:00	30	11.0	6.1
18 May 2012	6:44:00	30	11.0	6.8
19 May 2012	6:33:00	30	11.5	5.2
20 May 2012	7:38:30	30	6.0	7.6
21 May 2012	7:31:30	30	10.0	6.2
22 May 2012	6:28:30	30	12.0	5.7
13 March 2013	12:46:00	30	4.7	5.5

The coordinates of GW Lib ( $15^{\text{h}}19^{\text{m}}55^{\text{s}}$ ,  $-25^{\circ}00'25''$ ) allow it to be observed all night from Mt John in May. This coincided with a run of exceptionally good observing conditions, and enabled a total of 61 h of excellent quality photometry to be measured over 6 nights – an impressive 42 per cent observing duty cycle for these single-site runs.

Our next observation of GW Lib was not until March 2013, and by this time GW Lib had returned to a similar state as was seen in March 2012. A short run on 2012 June 24 using the Agile photometer on the 3.5 m telescope at Apache Point Observatory confirmed that the  $\sim 1100$  s modulation remained strong (P. Szkody, private communication). We are not aware of any other interim observations, so our best constraint on the length of time that the modulation was visible is three months to one year.

The 21 minute modulation was detected again during an observing campaign in April – May 2015. The analysis of these new data is ongoing, and results will be detailed in a future publication.

### 3 THE 1100 S PERIODICITY

The dominant feature of the May 2012 runs was a double-humped  $\sim 1100$  s (19 minutes) modulation. The DFTs for each night (Fig. 2; right panels) show an apparent frequency variation of tens of seconds between nights, and the April 23 run suggests that the variability range may be even larger ( $\sim 100$  s).

This appears to be the return of a modulation that was visible for at least four months in 2008 (Copperwheat et al. 2009; Schwieterman et al. 2010; Bullock et al. 2011; Vican et al. 2011). The shape and amplitudes have changed from the earlier observations: in 2012 we find a higher-amplitude (50 mma versus 22 mma) and non-sinusoidal double-humped modulation profile.

The origin of this period was not clear from the 2008 observations: Copperwheat et al. (2009) suggested that it could arise from accretion-based phenomena originating in the disk, but Vican et al. (2011) countered this by explaining that such quasi-periodic oscillations (Warner et al. 2003)

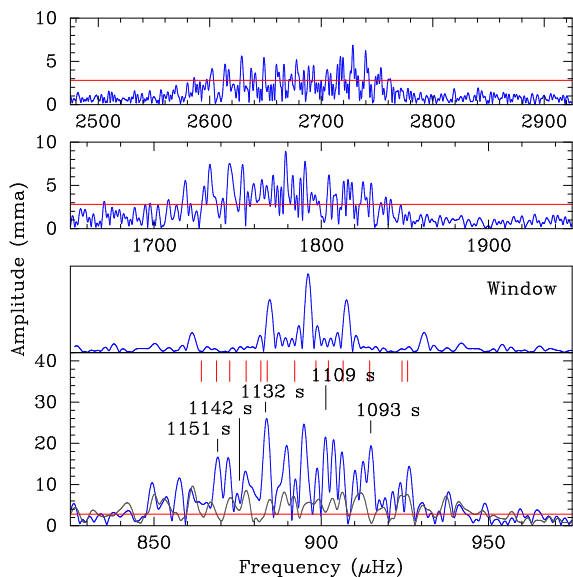


**Figure 3.** The combined DFT of the May 2012 runs is not consistent with stable pulsation modes. The DFT power in the vicinity of the main 19 minute periodicity (bottom panel) is dominated by five periods on top of a hump of less coherent power that requires a thirteen frequency fit (vertical red lines) to reduce below the 0.1 per cent FAP threshold (horizontal red line). The window function (upper-bottom panel; see text) shows the signature of the sampling aliases introduced by the daily gaps in the light curves. The harmonics (top panels) do not show any clear frequency structure.

are a characteristic of high accretion rate systems and aren't expected to occur in GW Lib. Instead they proposed that it may be a newly driven pulsation mode of the WD. The pulsation mode interpretation is strongly supported by our observations that show the modulation return in 2012 with a very similar period and behaviour.

It is a standard practice when observing the stable WD pulsators to combine multiple nights of photometry to improve the frequency resolution of the DFT. We attempt this for our May 17 – 22 observations in Fig. 3.

The main panel at the bottom of this figure presents the amplitude spectrum (blue) around the main periodicity, which resolves a messy comb of peaks that can be roughly fitted as the sum of five (simultaneously fitted) stable sinusoidal modulations. There is not a one-to-one correspondence between frequency peaks and periods because the daily gaps between runs creates an artificial modulation that introduces aliases separated by  $11.6 \mu\text{Hz}$  ( $1 \text{ day}^{-1}$ ). The signature of these aliases is illustrated by calculating the DFT of a noise-free sinusoid that is sampled at the the same times as the original data. This DFT *window* function is plotted for a 1100s sinusoid immediately above the bottom panel in Fig. 3.

The five-frequency fit does a poor job of reproducing the phases of the individual nightly light curves, and the amplitude shows beating effects that are not consistent with the data. These appear as a hump of power extending above the 0.1 per cent FAP threshold in the DFT of the residual signal (bottom panel; grey). A simultaneous thirteen-frequency fit (indicated with red lines in Fig. 3) is required to adequately describe the light curves in the time domain, but large beat-

ing effects remain visible in the gaps between runs. This is clearly not a realistic model.

These results show that the frequency variability of the modulation cannot be attributed to beating between a set of stable pulsation modes, so we conclude that the period(s) is/are truly variable in frequency and/or amplitude. This presents a problem for the standard model of pulsations that is applied to the slowly rotating isolated WDs – frequencies should change only over evolutionary timescales, not over hours. We know, however, that this assumption is not strictly true even for the isolated WDs: the cool DAV stars such as G29-38 (Kleinman et al. 1998) and the DBV star GD 358 (Kepler et al. 2003) show amplitude modulation, with power that shifts between different stable modes across observing seasons. The recent discovery of flaring DAV WDs (Bell et al. 2015; Hermes et al. 2015) provide a new class of WD pulsator that shows power shifting between modes in response to flare events that regularly repeat on a timescale of a few days.

### 3.1 Spectrogram analysis

A useful technique for visually depicting a multi-periodic signal that changes over time is the spectrogram (also known as a running Fourier transform). Spectrograms show a running plot of the DFT amplitude using colour over a range of frequencies against time. They are commonly used in audio signal analysis, but have also been applied to the study of pulsating WDs that exhibit amplitude variability (e.g. Hermes et al. 2015; Provencal et al. 2012).

The spectrogram extends the idea of dividing a signal into discrete chunks for comparison into a continuous process: each vertical slice in a spectrogram plot corresponds to the DFT amplitude calculated using data within a specified time window. The window is moved continuously across the data set in order to generate the plot. There is a trade off between frequency and time resolution: we chose a spectrogram window size of 3 h to give a reasonable time resolution while not sacrificing too much frequency resolution.

A spectrogram of the May 2012 data is presented in Fig. 4. No significant signals were found at frequencies above  $4200 \mu\text{Hz}$  (periods shorter than 240 s), and so this was chosen as the maximum frequency limit of the plot.

The harmonic frequencies are immediately apparent in the spectrogram at multiples of the strong fundamental frequency. The fundamental frequency can be seen to change over the course of each night, and this change is even more visible in the harmonics where the change is multiplied by the harmonic order. The first three runs show additional power near 285 s ( $3500 \mu\text{Hz}$ ) that does not follow the pattern of the 1100 s modulation; this appears to be the 280 s pulsation mode that was seen through the 2011 observations.

The runs on May 17, 18, and 21 appear to show step-changes in frequency (the step itself is blurred over the 3h window), while the May 19 and 22 runs show a more continuous wandering.

In an effort to obtain more quantitative results, the spectrogram was used as a guide to split each nightly run into two or three sub-runs, which were then individually re-analysed. Table 3.1 presents the details and periods found in each of these sub-runs.

The period uncertainties were calculated using a Monte

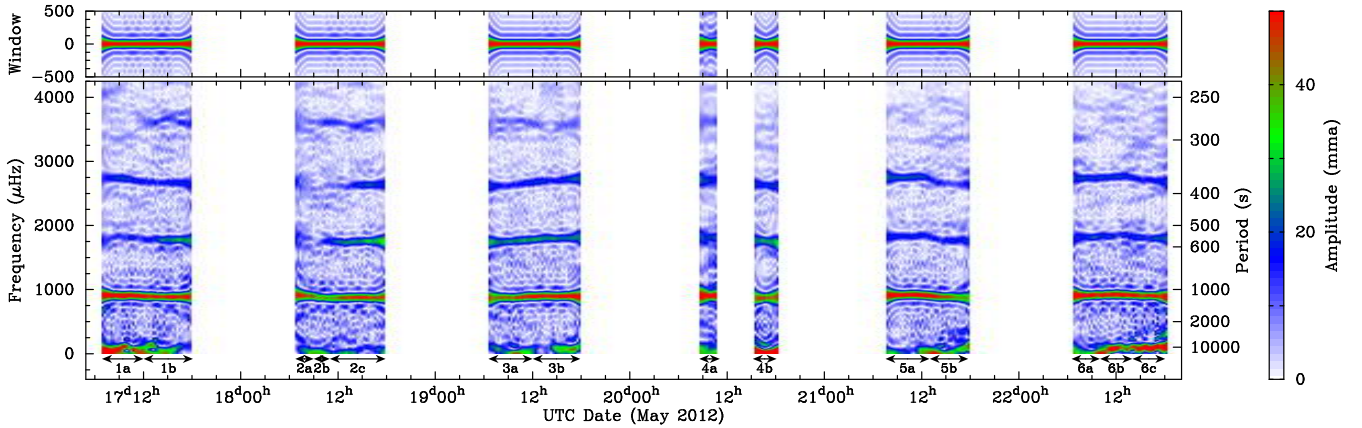


**Figure 4.** A spectrogram of the May 2012 runs shows how the modulation periods evolved over six consecutive nights in May 2012. The DFT amplitude of a three-hour segment of the data is plotted (using the colour-coded scheme given at the right of the figure) as a function of frequency and mid-segment time. The frequency resolution is indicated by the top panel which shows the spectrogram of a noise-free sinusoid sampled at the same times as the data (a direct analogue to the DFT window function).

**Table 3.** A summary of the complete May 2012 data set for GW Lib and the various periods deduced from nightly DFTs and multi-frequency fits to various sections of the time-series data.

UT Date (2012)	Sub run	Time span (UTC)	$\Delta t$ (h)	Period 1 (s)	Ampl. 1 (mma)	Period 2 (s)	Ampl. 2 (mma)
17 May	1a	06:53 – 12:00	5.1	$1108 \pm 1$	$52 \pm 2$		
	1b	12:00 – 18:06	6.1	$1133 \pm 1$	$50 \pm 2$	$276.8 \pm 0.3$	$25 \pm 2$
18 May	2a	06:43 – 09:00	2.3	$1114 \pm 18$	$52 \pm 3$		
	2b	09:00 – 11:00	2.0	$1176 \pm 80$	$33 \pm 2$	$280 \pm 1$	$14 \pm 3$
	2c	11:00 – 17:52	6.9	$1150 \pm 1$	$46 \pm 1$	$280.5 \pm 0.2$	$11 \pm 1$
19 May	3a	06:33 – 12:00	5.5	$1145 \pm 1$	$46 \pm 1$	$277.0 \pm 0.3$	$16 \pm 1$
	3b	12:00 – 17:55	5.9	$1119 \pm 1$	$50 \pm 1$		
20 May	4a	08:33 – 11:07	2.6	$1110 \pm 1$	$57 \pm 2$		
	4b	15:10 – 18:06	2.9	$1146 \pm 1$	$44 \pm 2$		
21 May	5a	07:32 – 13:00	5.5	$1096 \pm 1$	$51 \pm 1$		
	5b	13:00 – 17:46	4.8	$1137 \pm 1$	$47 \pm 2$		
22 May	6a	06:28 – 10:00	3.5	$1105 \pm 1$	$51 \pm 2$		
	6b	10:00 – 14:00	4.0	$1092 \pm 1$	$53 \pm 1$		
	6c	14:00 – 18:03	4.0	$1113 \pm 1$	$48 \pm 2$		

Carlo procedure: first the time-series data were pre-whitened by removing all the significant frequencies, a noise histogram characterising the residual variations was created, and this was fitted with a Gaussian. A synthetic lightcurve was computed using the modelled periods and random noise sampled from the fitted Gaussian, and then a new period determination for a specific period was made using a non-linear squares fit while holding the other periods fixed. Repeating this procedure 1000 times yielded histograms for the fitted period and amplitude values. Fitted Gaussian parameters from these histograms were used to obtain the stated period and amplitude uncertainties.

We note that this procedure measures only the uncertainty in fitting the data, and does not account for any systematic uncertainties that may be present. As such, they should be treated as lower limits.

We find that the sub-runs are each well described by a mono-periodic non-sinusoidal modulation, and that four of the sub-runs feature the 280s pulsation mode. Fig. 5 demonstrates the improvements that come from considering the individual sub runs by presenting light curves folded on the

$\sim 1100$ s periods (left panels), and DFTs (right panels) for the two May 19 sub-runs (bottom panels) and the full May 19 and April 23 runs (top panels) for comparison.

In both the April and May runs we see a clear double-humped profile, but the shape and relative phase of the humps differ. The profile shape does not show significant changes between the May sub-runs, but the best-fit periods change by as much as 30 seconds.

The bottom panel shows the result of folding the full May 19 light curve on its best-fit period. The phase profile is poorly defined compared to the two sub-runs, and there are significant residuals in the prewhitened DFT. This is quite a contrast to the sub-runs that it covers, which are individually more coherent and appear in their DFTs as a single well defined non-sinusoidal period.

#### 4 THE 280 SECOND PERIODICITY

Figure 5 shows an additional result: the  $\sim 280$ s pulsation is well defined in the May 19 1a sub-run, but indistinguishable

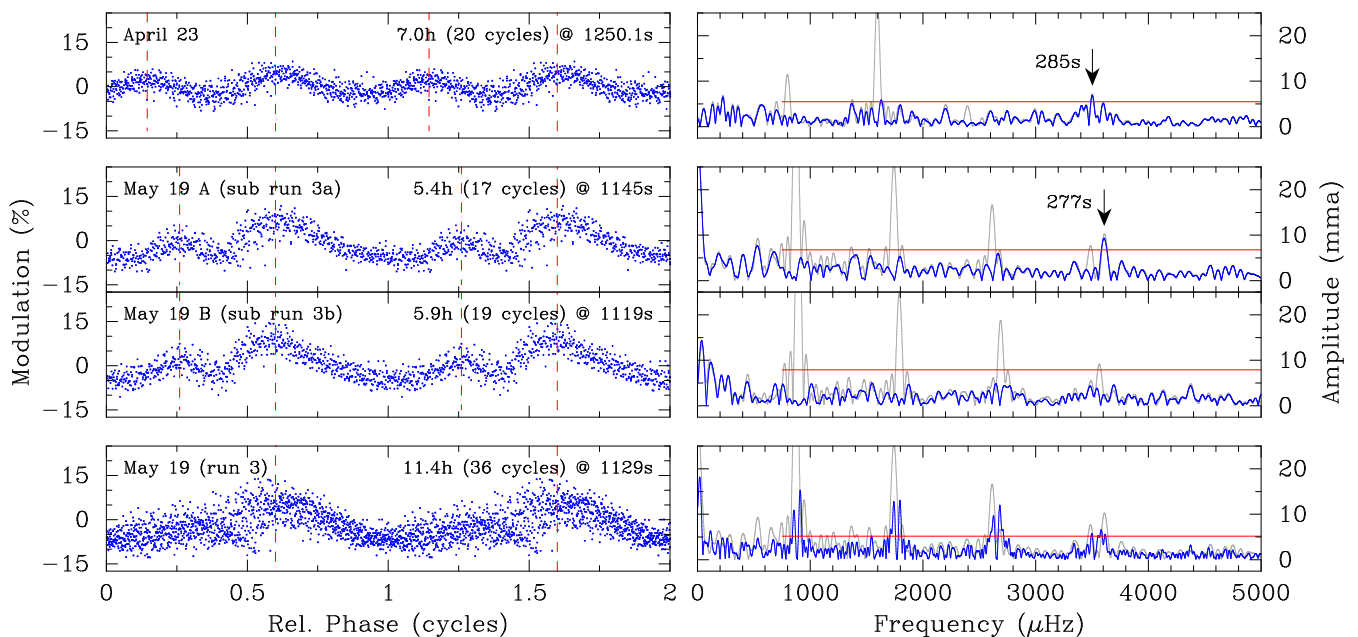


**Figure 5.** The short-term coherency of the 1100 s modulation is explored by presenting folded light curves (left panels) and DFTs (right panels) of the 2012 May 19 and April 23 runs. The  $\sim 3$  h modulation was first prewhitened from each run, and the data were then folded at the best-fit  $\sim 1100$  s period. The vertical lines in the folded light curve panels indicate the (arbitrarily aligned) phases of the modulation peaks. The right panels present DFTs before (grey) and after (blue) pre-whitening the best-fit modulation period indicated in the left panels. The horizontal lines in the DFT panels indicate the standard 0.1 per cent FAP threshold. See text for an interpretation of these plots.

from the noise in the 1b sub-run. Similar sharp changes are seen in the May 17 and 18 runs.

This suggests that the frequency multiplets reported in [Szkody et al. \(2012\)](#) are likely to be artefacts caused by amplitude and/or frequency variability. We test this idea by running a spectrogram analysis over our 2011 Mt John data, which is presented in [Fig 6](#).

The 2011 July 1, 2, 4 runs show similar wandering behaviour to the May 2012 1100 s periodicity: power appears to shift between temporarily stable frequencies. The 280 s mode is visible in the 2011 July 6 run, but the run length is too short to detect any changes. We see power in the expected region for the April 2012 run, but it appears to have relatively poor coherency.

## 5 THE 3 HOUR PERIODICITY

A  $\sim 3$  h modulation is visible by eye in the April and May 2012 light curves ([Fig. 2](#)), but the specific details of the modulation are masked by the  $\sim 19$  minute signal.

[Figure 7](#) presents pre-whitened light curves that provide a clearer view of the long period modulation. We find that this variability can be broadly described by beating between a 3.4 hour and a 2.8 hour signal, but, like the  $\sim 19$  minute modulation, significant residuals remain after prewhitening this model fit. We therefore consider it more likely that this behaviour is caused by a single quasi-stable modulation.

We find that our sub-run divisions (which were chosen empirically based on the behaviour of the  $\sim 19$  minute modulation) appear to coincide with discontinuities in this long period signal: the 1a/1b and 6b/6c run splits occur immediately before sharp increases in the modulation, and the

5a/5b and 6a/6b splits line up immediately before sharp decreases in the signal.

The spectrogram of the 2011 July 4 run ([Fig. 6](#)) shows a sharp change in the long-period signal that appears to be correlated with the change in the 280 s modulation. The DFT of the full run shows an apparent frequency triplet centred on 295 s, but when we split the night into two sub-runs based on the behaviour of the long-period modulation we find different best-fit periods of 293 s where the long period modulation is strong, and 297 s where it is weak (see [Fig 8](#)).

It is possible that these correlations are coincidental, but we consider it unlikely. Another example of this correlation can be seen in [Fig. 2](#) of [Tolozza et al. \(2016\)](#), which shows a UV light curve of GW Lib obtained over three HST orbits in 2013. Their light curve of the second orbit shows the 280 s pulsation appear with increasing amplitude on the rising slope of a strong long-period modulation. [Schwieterman et al. \(2010\)](#) also reported an apparent anti-correlation between the amplitude of the 2.1 hour and 19 minute signals in 2008. These results together suggest that a common mechanism is acting to affect the  $\sim 280$  s,  $\sim 19$  minute, and long period variability in GW Lib.

## 6 CONCLUSIONS

Observations of GW Librae over a three month period in 2012 showed the return of a  $\sim 1100$  s modulation period that was previously detected over several months in 2008. The fact that this returned with an essentially identical period, and its extended near-coherent modulation behaviour rule out the earlier speculation that this was a transient or quasi-periodic oscillation associated with the accretion disk.



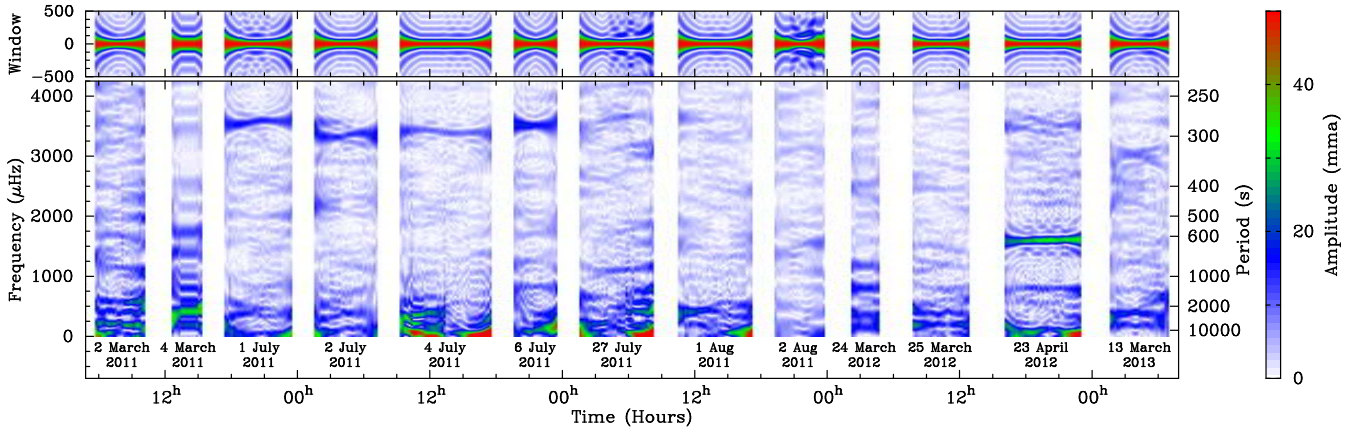


**Figure 6.** Spectrograms of the other Mt John runs reveal a similar wandering behaviour within the  $\sim 280$ s pulsation (near  $3400\mu\text{Hz}$ ). The disjoint runs have been combined on to a common time baseline for display purposes.

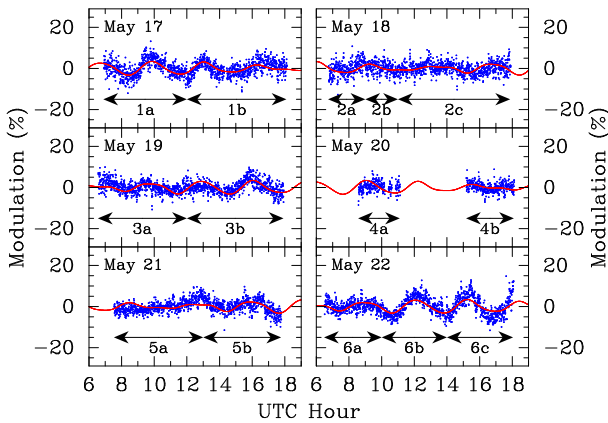


**Figure 7.** Pre-whitening the  $\sim 19$  minute and  $\sim 280$ s signals from the May 2012 light curves provides a clearer look at the  $\sim 3$  hour modulation. The best two-frequency model is shown in red, and the sub-run divisions are indicated below the data.

We find that the frequency variation cannot be described in terms of beating between stable pulsation modes, and that the period of a single mode appears to switch between quasi-stable values every few hours. Observations in March and April 2012 constrained the overall growth time of this modulation to less than two months, and suggested that the modulation showed large changes in period and the relative phase of the two humps during its growth.

We also track the behaviour of the  $\sim 280$ s pulsation mode where it is visible, and the long-period  $\sim 3$  hour modulation. We find that changes in the behaviour of these modulations appear to be correlated in time with changes in the behaviour of the  $\sim 1100$ s signal. We show a similar correlation in our previously published 2011 July 4 run, and note similar correlations that have been presented in two other papers.

The 280s mode has been clearly identified as pulsation behaviour on the WD (Szkody et al. 2012), and we can therefore infer that the  $\sim 1100$ s periodicity must also be a pulsation mode. This allows us to revise our estimate of when pulsations returned after the 2007 outburst from 2010 back to 2008.

The  $\sim 3$  hour modulation period has not been previously

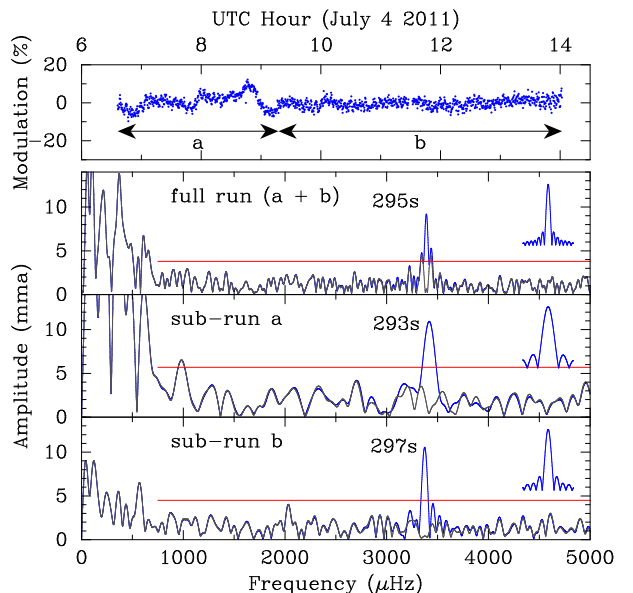


**Figure 8.** The 2011 July 4 run is split into two sub-runs at the point where the long-period variability changes character. The blue curves in the bottom three panels show the DFTs of the three data sets, and the grey curves show the DFTs after prewhitening the noted periods. The horizontal red lines show the 0.1% FAP thresholds. We find different best-fit periods for the  $\sim 280$ s pulsation mode in each sub run, and note that these periods cleanly prewhiten from the data. The DFT of the full run appears to show side-peaks around the best-fit period, which is a sign of the variability of the mode.

reported, but the modulation amplitude and quasi-periodic behaviour is consistent with the known  $2/4$  period modulation. We therefore believe that this is another state of the same modulation phenomenon for which we still lack a physical explanation.

The origin of the sharp changes in the pulsation behaviour remains a mystery, but there is observational evidence to suggest that this phenomenon is a general feature of the accreting pulsators:

- SDSS 0745+4538 (Mukadam et al. 2007) is another pulsating CV system, which features a double-humped  $\sim 1100$ s

period that was found to change by as much as 30 s between nights. This pulsation disappeared when the system went through an outburst in 2006, and later returned with the same periods and behaviour in 2010 (Mukadam et al. 2011).

- An extensive photometric data set on V455 And (Szkody et al. 2013) following its 2007 outburst reveals pulsation periods that drift over a wide range of values within certain allowed regions (B. Gänsicke, private communication).

- The three canonical pulsation periods that GW Lib showed before its 2007 outburst were also found to be unstable at the  $\sim \mu\text{Hz}$  level (van Zyl et al. 2004).

These period transitions pose a challenge for observing these systems, as it means that we cannot improve the signal to noise ratio in the DFT by extending the observation baseline – this simply introduces artefacts caused by the frequency and amplitude modulation. The spectrogram technique presented here provides a useful method for monitoring the stability of the pulsations if sufficiently high quality photometry is available.

Recent models of rapidly rotating pulsating WDs (Townsend et al. 2016) suggest that retrograde pulsation modes with periods close to the WD spin period may be slowed down to an apparent period of  $\sim$ hours in the observer’s frame of reference. This provides a convenient explanation for both the temporal correlation in the behavioural changes, and also for how the long-period mode can change between the observed 2/3/4 hour periods (a small wandering in the true period would be magnified to a large change in the visible period).

An alternative explanation for the correlation is that the long period signal is tracking large-scale changes in the WD atmosphere, which are then also perturbing the frequency and amplitudes of the observed pulsation modes.

The theory that the long period modulation is associated with the accretion disk appears to be ruled out by Toloza et al. (2016), who show that the modulation seen during the 2013 HST run was associated with temperature changes in the WD atmosphere.

The recent discovery of isolated DAV pulsators that undergo regular flare events (Bell et al. 2015; Hermes et al. 2015) may provide some insights into this behaviour. The pulsation modes that are visible during the flares have much higher amplitude and shorter period than the quiescent modes, but then all pulsation modes rapidly cease for a time, before growing back with the original quiescent periods. One proposed mechanism for this behaviour is that nonlinear coupling between pulsations cause power to be dumped into damped daughter modes. Similar nonlinear effects could be affecting the behaviour that we are seeing in GW Lib.

While we are making progress on untangling the observed behaviour of GW Lib and the other accreting pulsating WD systems, many questions and uncertainties remain. Further monitoring and modelling is required to sort out the details.

## ACKNOWLEDGMENTS

We thank the Marsden Fund of NZ for providing financial support for this research and the University of Canterbury for the allocation of telescope time for the project. PC acknowledges funding from the European Research Council under the European Union’s Seventh Framework Programme (FP/2007-2013) / ERC Grant Agreement n. 320964 (WDTracer). We also thank Boris Gänsicke and the anonymous referee for insightful feedback and discussions that improved the manuscript.

This paper has been typeset from a  $\text{T}_{\text{E}}\text{X}/\text{L}^{\text{A}}\text{T}_{\text{E}}\text{X}$  file prepared by the author.

## REFERENCES

- Althaus L. G., Córscico A. H., Isern J., García-Berro E., 2010, *A&ARv*, **18**, 471
- Arras P., Townsley D. M., Bildsten L., 2006, *ApJ*, **643**, L119
- Bell K. J., Hermes J. J., Bischoff-Kim A., Moorhead S., Montgomery M. H., Østensen R., Castanheira B. G., Winget D. E., 2015, *ApJ*, **809**, 14
- Bergeron P., et al., 2011, *ApJ*, **737**, 28
- Brickhill A. J., 1991, *MNRAS*, **251**, 673
- Bullock E., et al., 2011, *AJ*, **141**, 84
- Byckling K., Osborne J. P., Wheatley P. J., Wynn G. A., Beardmore A., Braito V., Mukai K., West R. G., 2009, *MNRAS*, **399**, 1576
- Chote P., Sullivan D. J., 2013, in Krzesiński J., Stachowski G., Moskalik P., Bajan K., eds, *Astronomical Society of the Pacific Conference Series Vol. 469, 18th European White Dwarf Workshop*. p. 337
- Chote P., Sullivan D. J., Montgomery M. H., Provencal J. L., 2013, *MNRAS*, **431**, 520
- Chote P., Sullivan D. J., Brown R., Harrold S. T., Winget D. E., Chandler D. W., 2014, *MNRAS*, **440**, 1490
- Copperwheat C. M., et al., 2009, *MNRAS*, **393**, 157
- Duerbeck H. W., Seitter W. C., 1987, *A&AS*, **131**, 467
- Dziembowski W., Koester D., 1981, *A&A*, **97**, 16
- Fontaine G., Brassard P., 2008, *PASP*, **120**, 1043
- Hermes J. J., et al., 2015, *ApJ*, **810**, L5
- Kato T., Maehara H., Monard B., 2008, *PASJ*, **60**, L23
- Kepler S. O., et al., 2003, *A&A*, **401**, 639
- Kepler S. O., et al., 2005, *ApJ*, **634**, 1311
- Kleinman S. J., et al., 1998, *ApJ*, **495**, 424
- Maza J., Gonzalez L. E., 1983, *IAU Circular*, **3854**, 2
- Mukadam A. S., Montgomery M. H., Winget D. E., Kepler S. O., Clemens J. C., 2006, *ApJ*, **640**, 956
- Mukadam A. S., Gänsicke B. T., Szkody P., Aungwerojwit A., Howell S. B., Fraser O. J., Silvestri N. M., 2007, *ApJ*, **667**, 433
- Mukadam A. S., et al., 2011, *ApJ*, **728**, L33
- Mukadam A. S., et al., 2013, *ApJ*, **771**
- Pavlenko E., 2009, *Journal of Physics Conference Series*, **172**, 012071
- Piro A. L., Arras P., Bildsten L., 2005, *ApJ*, **628**, 401
- Provencal J. L., et al., 2012, *ApJ*, **751**, 91
- Ringwald F. A., Naylor T., Mukai K., 1996, *MNRAS*, **281**, 192
- Schwieterman E. W., et al., 2010, *Journal of the Southeastern Association for Research in Astronomy*, **3**, 6
- Sullivan D. J., Chote P., 2015, in Dufour P., Bergeron P., Fontaine G., eds, *Astronomical Society of the Pacific Conference Series Vol. 493, 19th European Workshop on White Dwarfs*. p. 199
- Sullivan D. J., et al., 2008, *MNRAS*, **387**, 137
- Szkody P., Desai V., Hoard D. W., 2000, *ApJ*, **119**, 365

- Szkody P., Gänsicke B. T., Howell S. B., Sion E. M., 2002, *ApJ*, **575**, L79
- Szkody P., et al., 2010, *ApJ*, **710**, 64
- Szkody P., et al., 2012, *ApJ*, **753**, 158
- Szkody P., et al., 2013, *ApJ*, **775**, 66
- Templeton M., Stubbings R., Waagen E. O., Schmeer P., Pearce A., Nelson P., 2007, Central Bureau Electronic Telegrams, **922**, 1
- Thorstensen J. R., Patterson J., Kemp J., Vennes S., 2002, *PASP*, **114**, 1108
- Tolosa O., et al., 2016, MNRAS, submitted
- Townsley D. M., Arras P., Bildsten L., 2016, preprint, ([arXiv:1601.02046](https://arxiv.org/abs/1601.02046))
- Uthas H., et al., 2012, *MNRAS*, **420**, 379
- Van Grootel V., Fontaine G., Brassard P., Dupret M.-A., 2015, *A&A*, **575**, A125
- Vican L., et al., 2011, *PASP*, **123**, 1156
- Warner B., van Zyl L., 1998, in Deubner F.-L., Christensen-Dalsgaard J., Kurtz D., eds, IAU Symposium Vol. 185, New Eyes to See Inside the Sun and Stars. p. 321
- Warner B., Woudt P. A., Pretorius M. L., 2003, *MNRAS*, **344**, 1193
- Winget D. E., Kepler S. O., 2008, *Ann.Rev.Astron.Ap.*, **46**, 157
- Winget D. E., Robinson E. L., Nather R. E., Fontaine G., 1982, *ApJ*, **262**, L11
- Winget D. E., Sullivan D. J., Metcalfe T. S., Kawaler S. D., Montgomery M. H., 2004, *ApJ*, **602**, L109
- Woudt P. A., Warner B., 2002, *Ap&SS*, **282**, 433
- Woudt P. A., Warner B., 2011, *Ap&SS*, **333**, 119
- Yoon S.-C., Langer N., 2005, *A&A*, **435**, 967
- van Spaandonk L., Steeghs D., Marsh T. R., Parsons S. G., 2010, *ApJ*, **715**, L109
- van Zyl L., et al., 2004, *MNRAS*, **350**, 307